Proceedings of ICRC 2001: 1999 © Copernicus Gesellschaft 2001

ICRC 2001

Galactic magnetic field structure and ultra high energy cosmic ray propagation

S. O'Neill[1], **A. Olinto**[1], **and P. Blasi**[2,3]

[1]Department of Astronomy and Astrophysics, University of Chicago, Chicago, IL 60637, USA
[2]NASA/Fermilab Astrophysics Group, Fermi National Accelerator Laboratory, Batavia, IL 60510-0500, USA
[3]Osservatorio Astrofisico di Arcetri, Largo E. Fermi, 5, Firenze, Italy

Abstract. We consider the effects of the Galactic magnetic field on the propagation of ultra high energy cosmic rays (UHECRs). By employing two methods of trajectory simulation, we investigate the possibility that UHECRs are produced within the Galaxy with paths strongly influenced by the Galactic magnetic field. Such trajectories have the potential to reconcile the existing conflict between proposed local sources and isotropic UHECR arrival directions.

1 Introduction

As is well known, the Greisen-Zatsepin-Kuzmin (GZK) cutoff constrains detected UHECRs to have been produced in or near the Galaxy. Specifically, detected proton primaries with energies exceeding 5×10^{19} eV must have been produced within 50 Mpc of Earth, and nuclei propagation distances are constrained even further (Puget et al., 1976). The near-isotropy of detected UHECR arrival directions, however, suggests that Galactic source locations are not easily associated with the observed arrival directions. We attempt to reconcile these observations by examining the possibility that UHECRs are Galactic in origin, but consist of iron nuclei primaries with trajectories influenced by the Galactic magnetic field. It has been shown by Blasi et al. (2000) that MHD winds from young neutron stars are capable of Galactic production of iron primaries that fit the observed UHECR energy spectrum. Such a production mechanism implies that most source locations should be found within the Galactic disk. With this in mind, we propagate iron nuclei UHECRs through a realistic model of the Galactic magnetic field to investigate the possibility that Galactic sources and isotropic arrival directions are not mutually exclusive phenomena.

Correspondence to: S. O'Neill
(smoneil@oddjob.uchicago.edu)

2 Galactic Field Model

Following Stanev (1997) and Harari et al. (1999), we adopt a large-scale regular Galactic magnetic field associated with the spiral arms of the Galaxy. Specifically, we choose a bisymmetric even-parity field model (BSS-S) in which the field reverses direction between different spiral arms, but is symmetric with respect to the Galactic plane. The field strength in the plane, directed along the spiral arms, at a point (ρ, θ) in Galactocentric coordinates is given by

$$B_{sp} = B_0(\rho)\cos(\theta - \beta \ln(\rho/\rho_0)) \quad (1)$$

with $\rho_0 = 10.55$ kpc as the Galactocentric distance to maximum field strength at $l = 0^\circ$ with $\beta = 1/\tan p$, where the pitch angle is $p = -10^\circ$. The radial dependence of the field strength is given by

$$B_0(\rho) = \frac{3r_0}{\rho}\tanh^3(\frac{\rho}{\rho_1})\ \ \mu\mathrm{G} \quad (2)$$

where $r_0 = 8.5$ kpc is the Galactocentric distance to the sun and $\rho_1 = 2$ kpc is a smoothing factor that allows for $1/\rho$ behavior beyond 4 kpc from the Galactic center. The field equation in the Galactic plane is given by

$$\boldsymbol{B}(\rho, \theta, z = 0) = B_{sp}[\sin p\hat{\boldsymbol{\rho}} + \cos p\hat{\boldsymbol{\theta}}] \quad (3)$$

For this even-parity model, we introduce z dependence of the following form

$$\boldsymbol{B}_S(\rho, \theta, z) = \boldsymbol{B}(\rho, \theta, z = 0)\left(\frac{1}{2\cosh(\frac{z}{z_1})} + \frac{1}{2\cosh(\frac{z}{z_2})}\right) \quad (4)$$

where the values $z_1 = 0.3$ kpc and $z_2 = 4$ kpc reflect the scale heights of the field in the Galactic disk and halo, respectively. Figure (1) gives a graphical representation of this regular field model, clearly illustrating the field association with the spiral arms. Note that this model generates field values ranging approximately from $0 - 6\ \mu$G, with a value of $3\ \mu$G in the solar neighborhood.

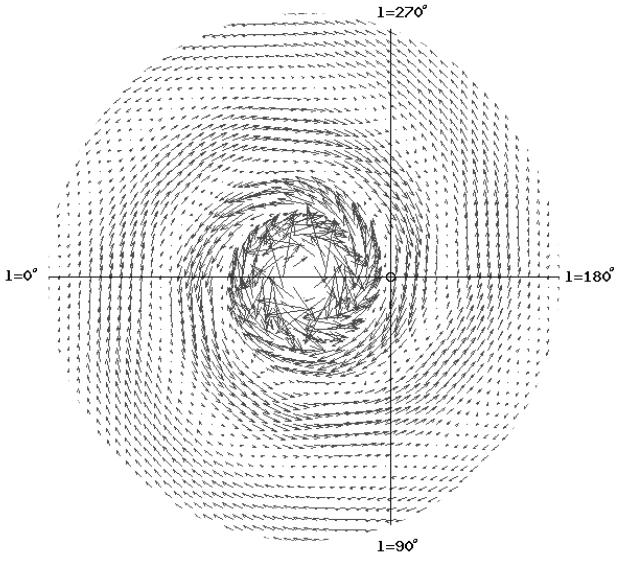

Fig. 1. Vector plot of the Galactic magnetic field. The solar position is shown at the intersection of the Galactic coordinate axes.

3 Simulations

We develop two distinct approaches to the simulation of Galactic UHECR trajectories. In our first method, we model a distribution of Galactic sources and emit UHECRs according to an assumed $N(E) \propto E^{-1}$ emission energy spectrum in order to study the arrival energy spectrum at a detector. This allows for comparison between the injected and observed energy spectrum. Our second approach consists of modeling the antiparticle trajectories as they depart Earth, given an assumed particle arrival spectrum. This is equivalent to plotting particle trajectories that are guaranteed to intersect Earth. This method allows us to investigate potential source locations for Earth-intersecting UHECRs in an attempt to discover expected anisotropies in UHECR arrival directions.

3.1 Particle trajectories

Our simulation of UHECR particle trajectories proceeds from a reasonable distribution of neutron stars within the Galactic disk to serve as injection regions for UHECRs. For simplicity, we assume that all sources are located in the Galactic disk of radius 25 kpc and thickness .65 kpc (taken from the scale height of the thin disk). We can derive a reasonable number of distinct sources from

$$N_{ns} = \frac{t_{int}}{r_{ns}} \tag{5}$$

where $t_{int} = 30$ Myr is the program integration time and $r_{ns} \simeq (1/100 \text{ years})$ is the neutron star birth rate. These values produce $N_{ns} = 300,000$ distinct UHECR sources. Given this set of sources, we assign a random time $t_{emit} < t_{int}$ at which each source emits randomly directed UHECRs according to the E^{-1} energy spectrum, chosen for its similarity to the UHECR arrival spectrum on Earth (Olinto, 2000). The particles then propagate through the Galaxy with paths influenced by the Lorentz force as they traverse the Galactic magnetic field.

Since an Earth-sized detector is too small to detect a significant number of events with computationally reasonable numbers of injections, we develop a series of larger detectors. The first is a 2D Galactocentric cylindrical detector of radius $r_0 = 8.5$ kpc, spanning 20-40 pc above the Galactic plane. The second detector is a 2D Galactocentric ring located 30 pc above the Galactic plane with an inner radius of 8.49 kpc and an outer radius of 8.51 kpc. These 2D detectors, placed at the solar distance from the Galactic center, possess a number of advantages over local 3D detectors by generating a much higher detection flux while simultaneously reducing the bias for detection of local sources.

With these detectors defined, we sample a number of UHECR energy spectra to compare the detected energy spectrum with the assigned E^{-1} injection energy spectrum. To accomplish this task, we inject millions of particles from our 300,000 sources and plot the detected energy spectrum. Figure (2) shows a typical detection energy spectrum from such a simulation. Since the energy emission spectrum is continuous, we bin the detected data before fitting it to a function of the form $N(E) \propto E^{-\alpha}$. For the data shown, we calculate $\alpha = .89 \pm .09$. This is well within 2σ of E^{-1}, so we find that the spectrum is not significantly changed for UHECRs. This is an important result since it is unknown *a priori* if the detection energy spectrum should reflect the emission spectrum when particles have the potential to be trapped in the Galactic field.

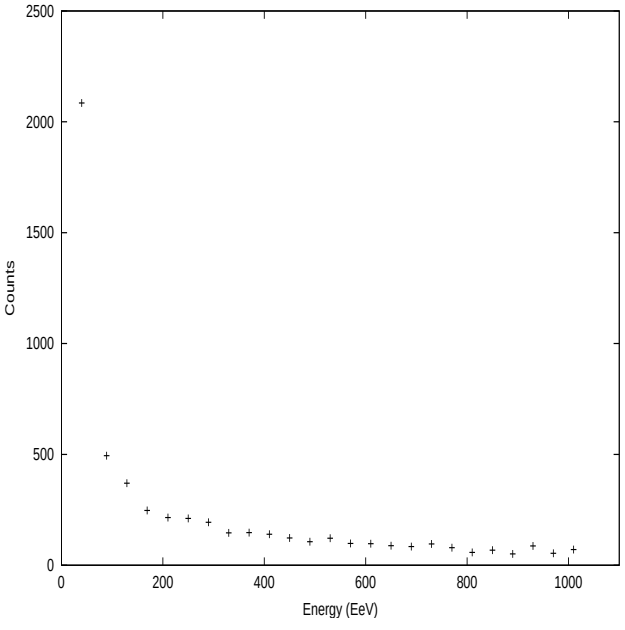

Fig. 2. Detected energy spectrum from particle simulations. Fit is of the form $N(E) \propto E^{-.89 \pm .09}$, matching the emission spectrum.

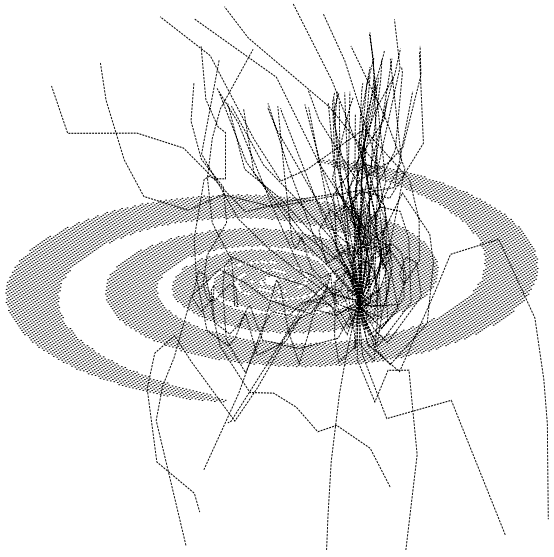

Fig. 3. 50 EeV antiparticle trajectories, emitted from Earth. The Galactic field is shown in the background for reference.

3.2 Antiparticle trajectories

This simulation addresses the other end of the UHECR problem, propagating anti-iron nuclei from a distribution of arrival directions at Earth. In this approach, we assign a specific energy to a set of emitted antiparticles and propagate them through the Galaxy to determine possible source locations for the corresponding UHECR particles. Figure (3) shows one such trajectory plot for the case of 50 EeV anti-iron. This method guarantees that our trajectories intersect Earth, but we are left to evaluate source location without an initial neutron star distribution. Keeping in mind the need for Galactic neutron stars as sources, we define a potential UHECR source location as any point along an antiparticle trajectory that intersects the Galactic disk. Furthermore, we closely examine those antiparticle trajectories for which the emission direction at Earth differs from the sky position of the source. These particular paths are the least likely to be easily identified with their Galactic sources, and their abundance would lend support to Galactic UHECR origins.

We proceed by first emitting a uniform distribution of anti-iron nuclei from Earth. To examine the extent to which these emission directions differ from the source locations, we define a deviation angle θ as the angular separation between the emission direction of a given antiparticle and the sky position of a possible source. We can then use a threshold deviation angle θ_{min} as our first criterion for selecting possible source locations. After selecting those points on trajectories that lie at least θ_{min} away from the emission direction in the sky, we further require that these points are contained in the Galactic disk, using the same disk parameters as before. We define a source location, then, as any point along an antiparticle trajectory that deviates at least an angle θ_{min} from the emission direction before leaving the Galactic disk or, in some cases, after reentering the disk. Selecting a sample angle $\theta_{min} = 10^{\circ}$, we find that the number and location of potential sources is strongly dependent upon the initial energies of the antiparticles, as expected. For instance, approximately 21% of the 50 EeV trajectories contained points that qualified as source locations, while only 4% of 300 EeV trajectories contained such points. Although it is interesting to examine the number of trajectories that contain source locations, it is more instructive to detail which specific paths admit source locations.

Figure (4) shows the set of 100 EeV anti-iron emission directions corresponding to trajectories that contain Galactic source locations. Equivalently, this is the set of directions from which we can expect to detect particle UHECRs emitted from the Galactic disk. As seen in Fig (4), there is a clear anisotropy in arrival directions in this case of 100 EeV iron, with the vast majority of arrival directions located at $b < 0$ in Galactic coordinates. Within the parameters of our Galactic field and source distribution, it is very difficult to produce an isotropic distribution of iron UHECR arrival directions at Earth. Even if we reduce θ_{min} to 5°, we are still unable to achieve an isotropic set of arrival directions for 100 EeV iron. The situation improves slightly with $\theta_{min} = 5^{\circ}$, but only for the lowest UHECR energies near 50 EeV.

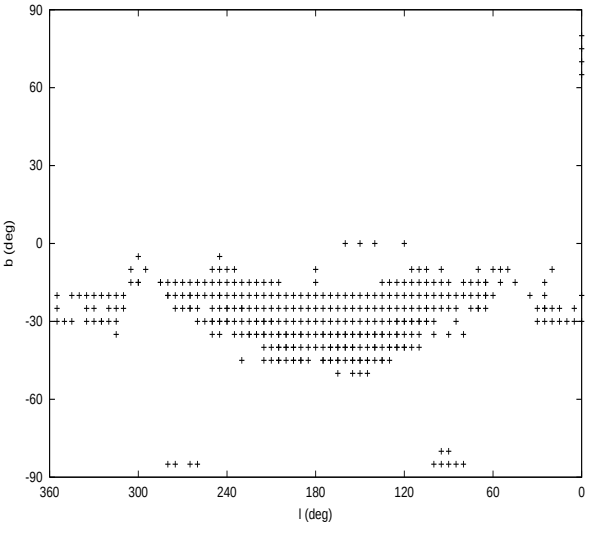

Fig. 4. Computed arrival directions for 100 EeV Iron, assuming source locations in the Galactic disk located at least $\theta_{min} = 10^{\circ}$ away from the arrival directions in the sky.

4 Discussion and conclusions

Needless to say, the results of both types of simulation exhibit sensitivity to certain parameters of the regular magnetic field model. Specifically, we find that variations in field strength strongly affect possible source locations for detected UHECRs. Figure (5) shows a contrast between the source location distributions for local field values of 3 and 6 μG.

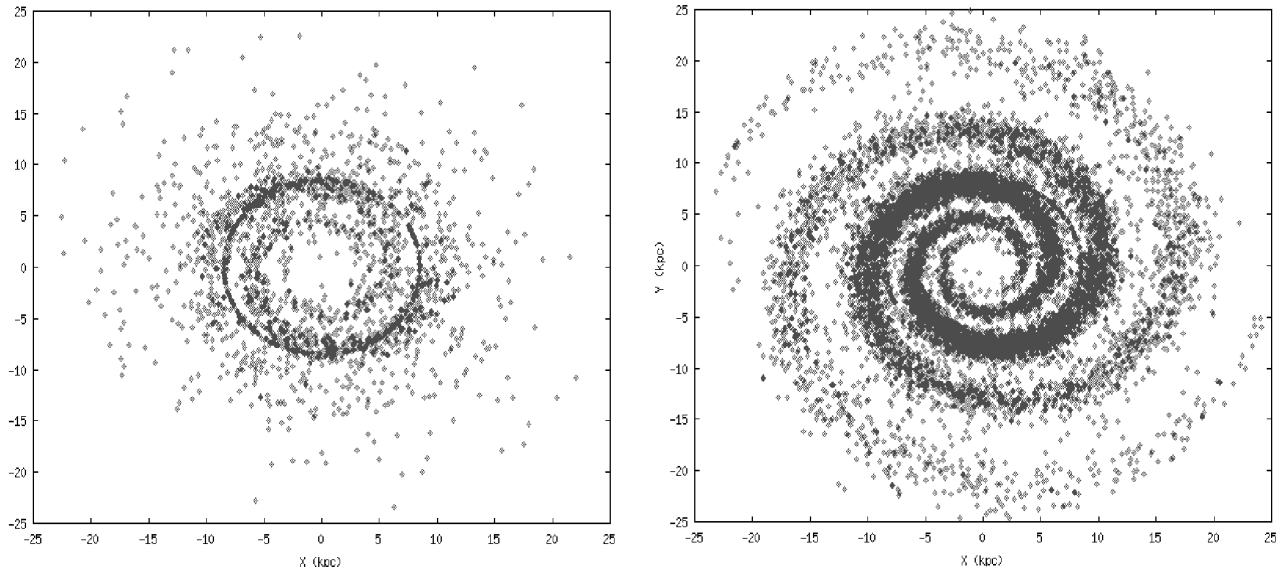

Fig. 5. Source locations for UHECRs using the Galactic cylindrical detector. The plot on the left shows locations for a 3 μG field (looking down at the Galactic plane) while the plot on the right is for a 6 μG field. For reference, the solar system is located at (8.5,0) in each picture.

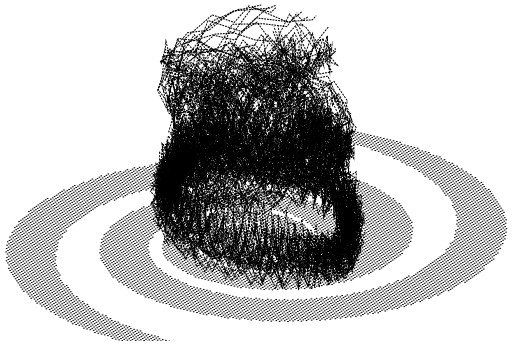

Fig. 6. Sample 100 EeV anti-iron trajectories through a proposed 7 μG Galactic wind field. The solar system is located in the lower right portion of the trajectories.

Clearly, the 3 μG field results in an abundance of detections involving local sources, while the 6 μG case exhibits pronounced non-local Galactic features in the detection spectrum. Furthermore, differences in the field strength do alter our results for possible anisotropies in the UHECR arrival spectrum. For the case of 100 EeV iron, the anisotropy is still very pronounced, but some lower energies begin to look more isotropic. For example, a 6 μG field with $\theta_{min} = 5^{\circ}$ generates a well-distributed set of arrival directions at 50 EeV. Clearly, our choice of field parameters is important.

Also, there are a number of proposed Galactic field components that, independent of the regular component, may greatly influence UHECR trajectories. For example, there is thought to be a significant Galactic wind, similar to the solar wind, that contributes strongly to the magnetic field of the Galaxy. Existing models of this field describe it as azimuthal with a local value as high as 7 μG (Ahn et al., 1999; Harari et al., 2000). Such a field configuration has the effect of establishing a detection bias for sources located north of the Galactic plane, as seen in Fig (6). Likewise, local high-field regions within the Galaxy have the potential to serve as scattering centers for UHECRs. A uniform Galactic distribution of these regions would have a diffusive effect on cosmic rays, further complicating the task of associating UHECRs with source locations. More accurate determination of Galactic field structure is needed before we can completely address the question of UHECR sources.

Acknowledgements. The work of A.V.O and S.O. was supported in part by DOE grant DE-FG0291 ER40606 and NSF grant AST 94-20759. The work of P.B. was supported by the DOE and NASA grant NAG57092.

References

Ahn, E.-J., Medina-Tanco, G., Biermann, P. L., Stanev, T., The origin of the highest energy cosmic rays Do all roads lead back to Virgo?, astro-ph/9911123, 1999.

Blasi, P., Epstein, R. I., and Olinto, A. V., Ultra-high-energy cosmic rays from young neutron star winds, Astrophys. J., 533, L123-L126, 2000.

Harari, D., Mollerach, S., and Roulet, E., The toes of the ultra high energy cosmic ray spectrum, astro-ph/9906309, 1999.

Harari, D., Mollerach, S., and Roulet, E., Magnetic lensing of extremely high energy cosmic rays in a galactic wind, astro-ph/0005483, 2000.

Olinto, A., Ultra high energy cosmic rays: the theoretical challenge, Phys. Rep., 333-334, 329-348, 2000.

Puget, J. L., Stecker, F. W., and Bredekamp, J. H., Photonuclear interactions of ultrahigh energy cosmic rays and their astrophysical consequences, Astrophys. J., 205, 638-654, 1976.

Stanev, T., Ultra-high-energy cosmic rays and the large-scale structure of the Galactic magnetic field, Astrophys. J., 479, 290-295, 1997.